Journal of ELECTRICAL ENGINEERING, VOL 73(2022), NO2, 108–115

sciendo

PAPERS

A novel principal component-based virtual sensor approach for efficient classification of gases/odors

Shiv Nath Chaudhri[1], **Navin Singh Rajput**[1], **Ashutosh Mishra**[2]

High-performance detection and estimation of gases/odors are challenging, especially in real-time gas sensing applications. Recently, efficient electronic noses (e-noses) are being developed using convolutional neural networks (CNNs). Further, CNNs perform better when they operate on a minimal size of vector response. In this paper, dimensions of the operational vectors have been augmented by using virtual sensor responses. These virtual responses are obtained from the principal components of the physical sensor responses. Accordingly, two sets of data are upscaled as a one-dimensional one. Another level of upscaling is further obtained by using the mirror mosaicking technique. Hence, with our proposed novel approach, the final vector size for CNN operations achieves a new dimension. With this upscaled hybrid dataset, consisting of physical and virtual sensor responses, a simpler CNN has achieved 100 percent correct classification in two different experimental settings. To the best of authors information, it is for the first time that an e-nose has been designed using a principal component-based hybrid, upscaled dataset and achieves 100 percent correct classification of the considered gases/odors.

K e y w o r d s: electronic nose (e-nose), gas sensor array, convolutional neural network (CNN), principal component analysis (PCA), zero-padding, mirror mosaicking

1 Introduction

Detection and estimation of gases/odors are gaining significant importance in real-time applications of electronic noses (e-Noses) in almost all the sectors of industry and society [1, 2]. Further details on e-Nose applications can be found elsewhere [3, 4]. The e-Noses are primarily developed by using pattern recognition methods including various statistical and probabilistic approaches or by using artificial intelligence (AI)-based methods like artificial neural networks (ANNs), convolutional neural networks (CNNs), deep networks (DNs), etc. by mimicking the human olfactory system. The statistical and probabilistic methods require full access to the dataset every time a new sample is tested, creating a bottleneck for its real-time application development [5]. For example, K-nearest neighbor (KNN) is a popular statistical method that requires the storage of training samples adding space complexity, and inhibiting real-time processing [6]. In contrast, AI-based approaches are best suited for real-time gas/odor classification application development [1, 2, 7]. A schematic diagram of an AI-based intelligent gas-sensing system (IGS) is presented in Fig. 1(a). It can be observed that the raw sensor array responses are first pre-processed for statistical normalization. Pattern recognition techniques are then applied to this normalized data for suitable detection and estimation of gases/odors. Furthermore, our proposed AI-based IGS utilizing hybrid analysis space has been shown in Fig. 1(b).

In an IGS, the gas sensor array responses are captured both in their transient and steady states. Normally, a sensor array consists of 4 to 16 gas sensor elements [8–13]. Recently, efficient e-Noses are being developed using convolutional neural networks (CNNs).

Peng *et al* (2018) have implemented a 2D Deep CNN to classify four gases/odors (Carbon Monoxide, Ethylene, Hydrogen, and Methane) [6]. Their proposed network "GasNet" is very complex and comprises 38 layers. Their classification accuracy is 95.20 % while each sample is an 8×1000 sized-input vector and they have used a total of 1200 vectors for designing the network. Further, Wei *et al* (2019) have developed a 2D-CNN to classify Carbon Monoxide, Methane, and its mixture [14]. Their proposed 2D-CNN is an augmentation of LeNet-5 (image processing CNN) [15] for gas/odor classification which achieves a classification accuracy of 98.67 % using 1000 vectors, with each sample having 12×480 elements. In another experiment, Han *et al* (2019) have detected three gases/odors (Carbon Monoxide, Ethylene, and Methane) and their two binary mixtures [13]. They achieved a classification accuracy of 96.67 % by using an 8×3000 sized-input sample vector in their dataset comprising of 540 sample vectors. In the aforesaid works, the authors have presented the data in 1D or 2D vectors. Interestingly, in these pioneering papers, the input sample vector achieves a high dimension due to the high sampling rate to sample each event of gas-sensor array exposure. Whereas the steady-state responses of metal oxide (MOX)-based non-selective sensors to respective analyte can only the considered as the golden response of a gas

[1] Department of Electronics Engineering, Indian Institute of Technology (BHU), Varanasi, 221005, India, [2] School of Integrated Technology, Yonsei University, South Korea,* Corresponding author: nsrajput.ece@iitbhu.ac.in

https://doi.org/10.2478/jee-2022-0014, Print (till 2015) ISSN 1335-3632, On-line ISSN 1339-309X

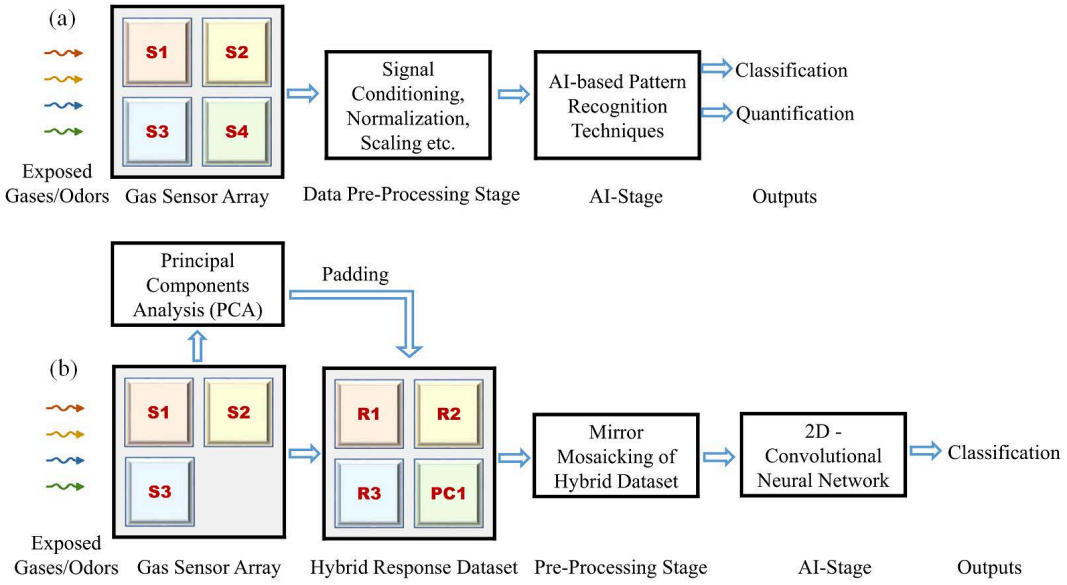

Fig. 1. (a) – AI-based intelligent gas-sensing system, (b) – AI-based IGS utilizing proposed hybrid analysis space

sensor array [16, 17]. Further, in real-field applications capturing transient response is impractical because the gas sensor array is continuously exposed to varying concentrations of various analytes. It can now be observed that in the above-referred publications the authors have used transient as well as steady-state responses making the input sample vectors to be a high dimensional vector with much less utility. Further, because of the large input sample vectors, corresponding CNN architectures are also deep and complex [6, 13–15]. Although, in recent publications simpler hybrid CNNs using analysis space transformation at the data preprocessing stage called drift tolerant robust classifier (DTRC) have also been reported as efficient gas/odor classifiers [18].

In contrast, in our proposed novel approach, we have optimally reduced the size of input sample vectors by taking the average of steady responses of the sensor array. This approach reduces the size of the input sample vector from $8 \times 600 \times 100$ to 8×1 and $5 \times 300 \times 25$ to 5×1, respectively. Further, considering that CNNs have the inherent capability to automatically extract more information if simpler one-dimensional (1D) data is upscaled in the form of multidimensional (2D or 3D) data structures. Accordingly, Table 1 shows the dimensions of intermediate stages of the input sample vectors during the proposed process of upscaling. It can be seen that the process of upscaling has two distinct processes viz., non-zero virtual sensor response-based data padding, and mirror mosaicking-based upscaling.

2 Proposed approach

In this section, details of our proposed approach have been presented under specific headings.

2.1 Gas sensor array response characteristic

Typically, a MOX-based gas sensor array consists of multiple gas sensing elements with varying characteristics. Such elements are produced by doping the base material of the sensor element with different dopants. The gas sensor array is interfaced with a data acquisition unit capable of sampling the responses at a very high frequency. The response of an activated sensing element to the exposing analyte is shown in Fig. 2.

Table 1. Intermediate dimensions of input sample vector in proposed upscaling process

Raw sample vector size ($N \times S_d \times S_r$)	Averaged steady responses	Padding virtual sensor responses	Squared shape of sample vector	Mosaicked sample vector
$8 \times 600 \times 100$	8×1	9×1	3×3	9×9
$8 \times 600 \times 100$	5×1	9×1	3×3	9×9

N - Number of physical gas sensors

S_d - Sampling duration (s), S_r - Sampling rate (Hz)

It can be observed that the sensor element response shows a significant drop in its characteristic resistance which is proportional to the affinity of the analyte with the sensing element and the analyte samples concentration called the transient response of a gas sensor element. Further, after some time the sensor element response arrives at a steady value of resistance change, usually measured in terms of percentage change in resistance called a steady-state response of a sensor element. While transient responses contain certain useful information about the class and respective sample concentration of the analyte,

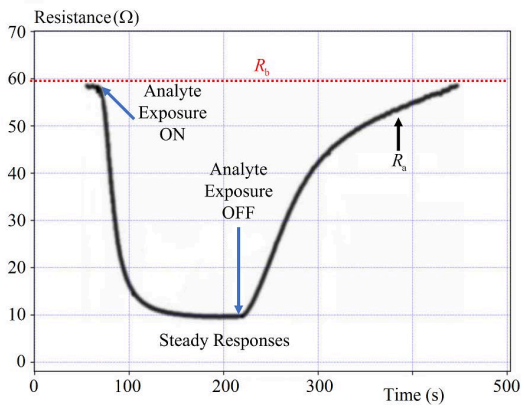

Fig. 2. Response curve of an activated MOX-based sensing element during the exposure of analyte

steady-state responses are the actual representative of the analyte which is truly proportional to the respective class and concentration of the sample. Steady-state responses are normally called gold responses of a gas sensor array and contain most of the overall information when compared with the transient responses. Accordingly, in the considered dataset available publicly, we have first extracted steady-state values from each of the 640 and 58 samples, respectively. In this way, the large input sample vector for each sample is downsampled from $8 \times 600 \times 100$ to 8×1 and $5 \times 300 \times 25$ to 5×1, respectively.

2.2 Upscaling of the input sample vectors

CNNs have the inherent capability to automatically extract more information if simpler 1D data is upscaled and presented to the CNN, in the form of 2D or 3D data structures. The input sample vectors obtained from the gas sensor array can be upscaled by using the popular mirror mosaicking technique [8]. However, mirror mosaicking requires the input sample vector in the form of a 2D-squared data structure as shown in Fig. 3. Further, every 1D data cannot be restructured as a 2D-squared data structure until the number of elements in the 1D data vector is a perfect square. Hence, if the sensor array response vector is not a perfect square, additional vector elements can be padded to make the 1D data to its nearest perfect square. Routinely, zero-padding has been quite popular for various padding-based purposes [19–22]. However, zero-padding does not contribute to information addition. Therefore, in this paper, we have demonstrated a novel approach for non-zero padding. In our proposed approach, we have padded additional information vector elements to the physical vector elements, in the form of non-zero virtual sensor response-based padding.

2.3 Virtual sensor responses

Mirror mosaicking inherently requires the input sample vector in the form of a 2D-squared data structure. However, the vector dimensions of raw gas sensor array responses depend on the number of physical gas sensor elements. If this physical sensor response vector is not a perfect square, it cannot be restructured as a 2D squared input sample vector. Hence, from the real physical sensor responses, additional information is further generated called the "virtual sensor response element" by using a variety of techniques as reported in [23]. These virtual elements are then appended with the real physical sensor response vector until the newly formed sensor response vector becomes a perfect square. A sensor response vector, consisting of real sensor responses and virtual sensor responses is called "hybrid sensor responses". Depending on the need, more virtual elements are appended to reach a perfect squared number. The process of virtual sensor response padding and its restructuring into a 2D-squared data vector is shown in Fig. 3.

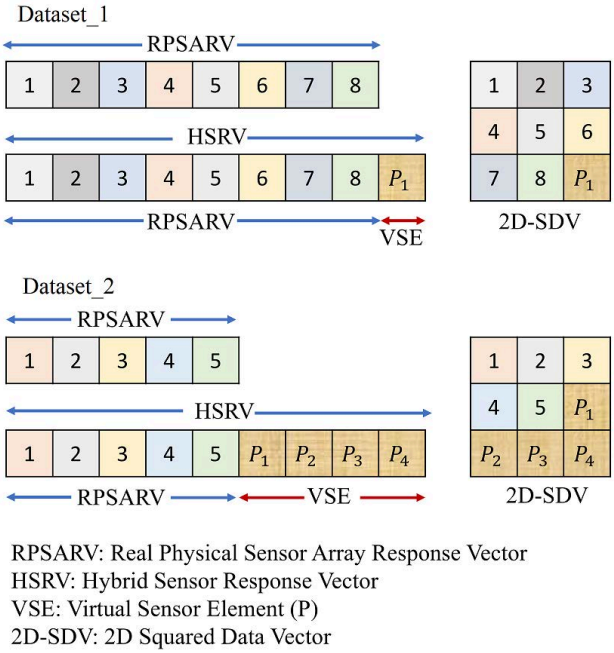

Fig. 3. A schematic showing procedure of non-zero virtual sensor response padding and 2D squared data vector

It can be observed that the two considered dataset_1 and dataset_2 have been first padded with a non-zero virtual sensor element, to make the input sensor response vector a perfect square, in the form of a hybrid vector. This 1D hybrid data, which is now a perfect square is then restructured as a 2D squared data vector.

2.4 Zero and non-zero padding

A generalized algorithm for non-zero padding can be explained as follows. Let us assume, the responses have been captured using a gas sensor array consisting of n gas sensor elements. Hence, the corresponding response dataset has n data points in each of the samples resulting from physical gas sensor elements. In this scenario, the following two cases arise:

1) If n represents a perfect square number, no padding of virtual sensor response is required. Since n can already

be denoted as $x\times = x$ where x represents a positive integer.

2) If n does not represent a perfect square number, some virtual sensor responses are needed to pad in the physical sensor responses because n cannot be denoted itself as $x \times x = n$ where x is a positive integer. In this scenario, we need to pad $(p-n)$ virtual sensor responses, where p is the smallest perfect square number such that $p > n$. After padding the required number of virtual sensor responses, p can be denoted as $y \times y = p$, where y is a positive integer.

The non-zero virtual sensor responses as required to make the hybrid sensor response vector, a perfect square, are generated from the physical sensor response vector itself [23]. The effectiveness of the so produced virtual sensor responses depends on the technique used. For example, with our proposed novel approach, a four-element physical sensor response can be appended with four more vector elements, by obtaining four principal components from the dataset, for use as virtual sensor responses. Principal Components Analysis (PCA) is a very effective technique for dimensionality reduction and data compaction through its principal components. Its principal components retain all the information a dataset has and only a few components can retain almost 95% of the total information contained in the raw data set on which PCA has been applied [24]. In our proposed method, we have utilized this property of PCA for the generation of virtual sensor responses. In our novel approach, the virtual sensor elements are also true representatives of the physical sensor responses Hence, a CNN when trained using such a hybrid sensor response used in a 2D or 3D format, performs with very high efficiency.

A detailed mathematical description of the process of PCA application is presented as follows. Let X be a dataset consisting of N number of observed samples for S variables. Here, each element in this dataset can be denoted as $x_{i,j} : \forall i = 1, 2, \ldots, N : j = 1, 2, \ldots, S$. This data matrix is adjusted by subtracting the mean of each variable to be centered about the origin. For the aforesaid purpose, we calculate the mean for each variable $\mu_j : \forall j = 1, \ldots, S$. After subtracting the corresponding mean from each column, we get origin centered data matrix X' where $x'_{i,j} = x_{i,j}$. Later, the covariance matrix of this centered data matrix X' is obtained as $C'_X = 1/(N-1)X : \forall {X'}^{\top}$. Determine the eigenvalues and eigenvectors of this covariance matrix, and sort the eigenvalues in descending order. Arrange the eigenvectors of the D sorted eigenvalues in column-wise fashion so that we get a matrix V where each element is represented as $v_{i,j}$ Thus, we get a projection matrix V consisting of independent D eigenvectors. The desired PCs can be calculated by projecting the centered data matrix on the obtained projection matrix. The corresponding PCs are achieved as

$$PC_i = x'_{i1}\, v_{i1} + x'_{i2}\, v_{i2} + \cdots + x'_{ij}\, v_{ij}\,, \qquad (1)$$

where: $\forall x'_{i,j} : i = 1, \ldots, N$ and $\forall v_{i,j} : i = 1, \ldots, S$, $j = 1, \ldots, D$.

The obtained PCs as our requirement are then padded in physical sensor responses considering virtual sensor responses. Thus, each sample in the resulting hybrid dataset is converted into a 2D squared input sample vector. Further upscaling of the samples is obtained by using the mirror mosaicking technique.

2.5 Mirror mosaicking

Mirror mosaicking is a popular sample upscaling technique [8, 25]. For sample upscaling, the 1D hybrid sensor response vector is first restructured as a 2D-squared data vector. This 2D-squared data vector is then flipped over its eight directional axes viz. W-E-N-S-NW-SE-SW-NE. Hence, in a 2D space, we get eight possible orientations to flip the primary 2D-squared data vector resulting in eight mirror images, as shown in Fig. 4(a).

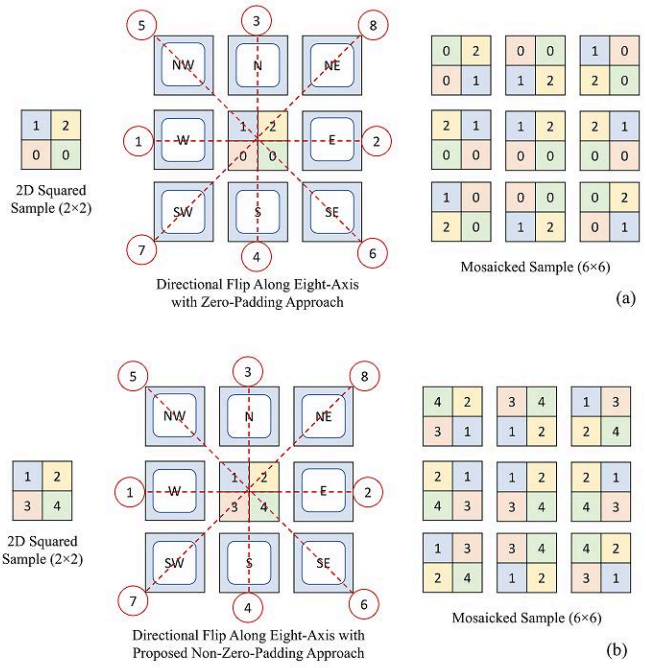

Fig. 4. Mirror mosaicking procedure showing with: (a) – zero-padded virtual sensor responses, (b) – non-zero-padded virtual sensor responses

In other words, the corresponding eight images are obtained by flipping the primary 2D-squared data vector, held at the center, along each of the eight axes. Later, these mirror images are mosaicked together to form a large-sized upscaled hybrid 2D-squared data structure. It can be observed that the mosaicked vector is now upscaled by three times than its primary 2D-squared vector. Interestingly, each element of the upscaled 2D-squared data vector, carried a good amount of information than the zero-padded situation, if used, as shown in Fig. 4(b). Figure 4 illustrates the mirror mosaicking technique with the help of a 2D-squared data structure having a 2×2 dimension. Here, 1, 2 are regarded as physical sensor responses and 3, 4 as virtual sensor responses, respectively.

Table 2. Hyperparameters of used simpler 2D-CNN

2D-CNN layers	Labels of hyperparameter	Hyperparameter value
Input Layer 1	Input dimension	$9 \times 9 \times 1$
Conv layer 2	Kernel/filter size	3×3
	No. of kernels	8
Conv layer 3	Kernel/filter size	3×3
	No. of kernels	16
Fully connected /Dense Layer 4	Number of neurons	32
Output Layer 5	Output Classes	4
Optimizer	Adam	Learning rate 0.001

2.6 2D convolutional neural network (2D-CNN)

The 2D-hybrid input sensor responses so generated are used to train and test a CNN for gas/odor classification. As presented earlier, we have two different datasets viz. dataset_1 and dataset_2. Both the datasets are upscaled in the 9×9 vector size. The general architecture of a CNN is presented in Fig. 5(a). It comprises multiple convolutional and pooling layers.

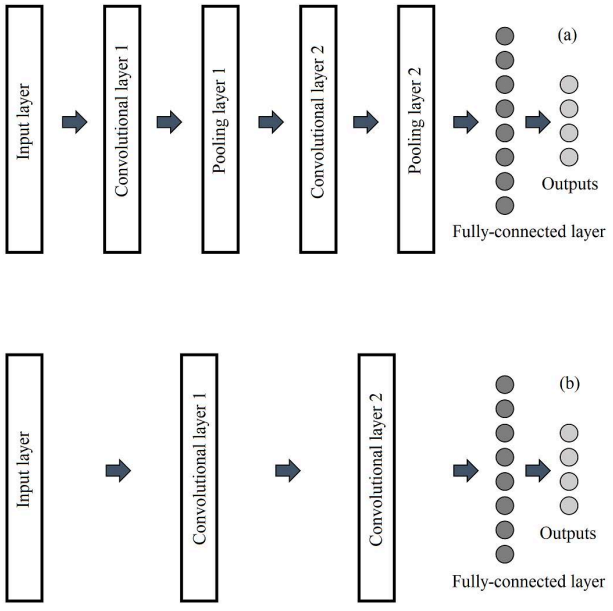

Fig. 5. (a) – General architecture of a CNN, (b) – architecture of the proposed CNN

Further, in the general architecture, it can be observed that a pooling layer is also used, especially for image processing applications, because adjacent pixels bear correlated information based on the information it carries. In contrast, in a gas sensor response system, steady-state responses of any two samples are mutually independent and the pooling layer does not serve any purpose. Hence, in our proposed novel architecture, we have simplified the CNN as shown in Fig. 5(b). It can be observed that the proposed architecture is much simpler and takes in a large multidimensional 2D- hybrid input sensor response vector with each element bearing significant information due to the non-zero PCA-based virtual sensor response approach. Considering that the input response to the CNN is hugely informative, the chosen CNN architecture consists of 5 layers only. Next to the input layer, we have used a pair of convolutional layers each followed by a pooling layer. Subsequently, the received final outputs from the previous layers are flattened to pass them into a fully connected layer. Eventually, the output of the fully connected layer is then passed through the softmax layer to provide the final classification results for the considered gases/odors. The hyper-parameters as used, have been given in Tab. 2.

3 Experimental results and discussion

3.1 Gas sensor array response data

In this work, the first dataset (dataset_1) has been taken from an open-source machine learning dataset repository [26]. It consists of transient responses of four considered gases/odors, Carbon Monoxide (CO), Ethanol (C_2H_5OH), Ethylene (C_2H_4), and Methane (CH_4) at different sample concentrations (CO: 25-250 ppm, C_2H_5OH: 12.5–125 ppm, C_2H_4 : 12.5 − 125 ppm, and CH_4 : 25 − 250 ppm). In this dataset, a gas sensor array with eight MOX-based gas sensor elements has been used. It consists of a total of 640 samples (160 samples of each gas/odor), while each sample is a time-series sensor array response captured over 600 seconds at a sampling rate of 100 Hz [27]. A ten-fold cross-validation data with a ratio of 80 % and 20 % for training and testing purposes have been respectively used. Accordingly, dataset_1 consists of 512 training (133-carbon monoxide, 127-ethanol, 131-ethylene, 121-methane) and 128 testing samples (27-carbon monoxide, 33-ethanol, 29-ethylene, 39-methane), respectively.

In this paper, we have also used another dataset for an exhaustive assessment of our proposed method. The second dataset has also been taken from an open-source machine learning dataset repository [26]. The dataset_2 has been captured using a 16-element MOX gas sensor array, using five different TGS-brand of gas sensors from Figaro Inc.

Table 3. TGS sensor elements in the referred gas sensor array

New/old
1/1
2/3
3/4
4/6
5/8

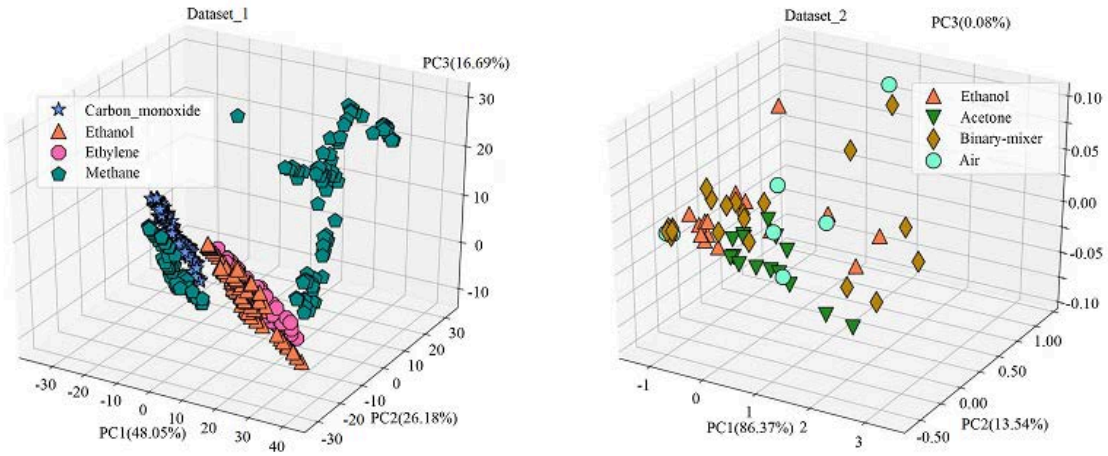

Fig. 6. Gases/odors cluster representation for both datasets

Construction details of this 16-element gas sensor array are given in Tab. 3. It can be observed that this sensor array has been constructed by using five different sensors, which are then used repeatedly to form the said 16-element gas sensor array. The sensor array responses are then captured by exposing the array with two types of gases *viz* ethanol and acetone and its binary mixer. Further, ambient air has been considered as the fourth class in this dataset. Accordingly, rather than using all the responses from the 16-elements of the sensor array, we have only taken the sensor data from five different sensors only. Hence, dataset_2 is the curated dataset on which we have applied our proposed method and achieved excellent results, even without using the whole data set available in the referred open database. The extracted dataset has a total of 58 samples of different concentrations of the considered gases, *viz* 15-ethanol, 15-acetone, 20-binary_mixer, and 8-ambient air. Further detail about this dataset can be found in [28]. We have further segregated the dataset_2 into a training dataset (39 samples) and a testing dataset (19 samples).

The scatter plots of both the datasets *viz* dataset_1 and dataset_2 have been shown in Fig. 6. Using the first three PCs we plot the clusters in a 3D space. It can be observed that different gases are well separated in different classes, although they have a significant amount of overlapping. The used PCs collectively explain 90.92 % variance (PC1: 48.05 %, PC2: 26.18 %, PC3: 16.69 %) for dataset_1, and 99.99 % variance (PC1: 86.37 %, PC2: 13.54 %, PC3: 0.08 %) for dataset_2. Both the datasets show overlapped clusters which inevitably pose a challenge to classify the considered gases/odors.

3.2 Approach implementation on the considered datasets

The dataset_1 has eight physical sensor responses requiring one virtual sensor response to implement the proposed approach. On the other hand, dataset_2 has five physical sensor responses. Here, we need four virtual sensor responses, accordingly. For both the datasets, only the average of steady responses has been used to classify the considered gases/odors. Henceforth, each dataset consists of nine hybrid responses (physical sensor responses and padded virtual sensor responses). Now, each hybrid dataset can be restructured in a 2D-squared sensor array response of 3×3 dimensions. With our proposed method, each hybrid sample is further upscaled to a 9×9 dimension. The flowchart is given in Fig. 7. presents the workflow of the proposed methodology for efficient classification of the considered gases/odors using a simpler 2D-CNN.

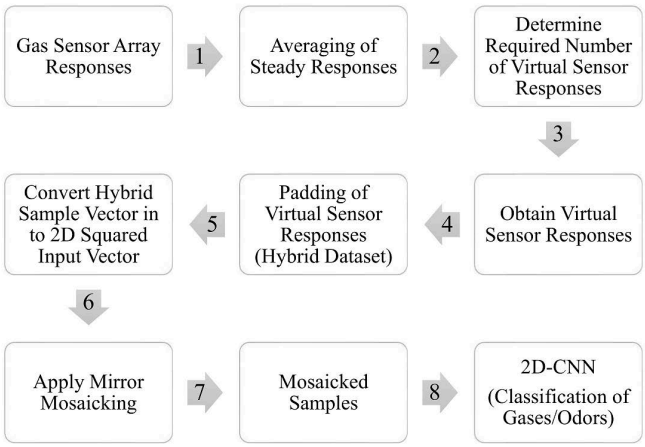

Fig. 7. Flowchart of the proposed approach

4 Results and discussion

The designed simpler 2D-CNN has been used, both for the datasets with the same hyperparameters. We have 128 and 19 unknown test samples respectively for dataset_1 and dataset_2. With our proposed approach, we achieved 100 % classification accuracy for both datasets. Thus, the obtained performances prove the efficacy of our proposed approach while classifying the considered gases/odors using a simpler 2D-CNN. Also, the performance of our pro-

Table 4. Performance comparison

	Physical Response /virtual response	Zero-Padded virtual responses	PCs -padded virtual responses	Enhanced performance
Dataset_1	8/1	1	1	-
OCA (%)	-	96.88	100	3.12
K	-	0.96	1.0	0.04
MSE	-	1.41×10^{-2}	7.75×10^{-3}	6.35×10^{-3}
Training time (s)	-	19.232	23.855	-
Dataset_2	5/4	4	4	-
OCA (%)	-	94.74	100	5.26
K	-	0.93	1.0	0.07
MSE	-	5.40×10^{-2}	4.20×10^{-2}	1.20×10^{-2}
Training time (s)	-	1.027	1.133	-

posed approach has been compared with the baseline performance obtained while using zero-padded virtual sensor responses. In these scenarios, the achieved performance for gas/odor classification has been presented in Tab. 4.

The obtained performance have been presented in terms of three performance metrics *viz* overall classification accuracy (OCA), kappa coefficient (K), and mean squared error (MSE). These metrics have been given in Tab. 4. The associated mathematical expressions to these performance metrics are denoted as

$$\mathrm{OCA} = \frac{\sum_{i=1}^{C} G_{ii}}{\sum_{i,j=1}^{C} G_{ij,i\neq j}}, \tag{2}$$

$$\mathrm{K} = \frac{N\sum_{i=1}^{C} G_{ii} - \left(\sum_{i=1}^{C} G_{i,\mathrm{act}} G_{i,\mathrm{pred}}\right)}{N^2 - \sum_{i=1}^{C} G_{i,\mathrm{act}} G_{i,\mathrm{pred}}}, \tag{3}$$

$$\mathrm{MSE} = \frac{1}{N}\sum_{i=1}^{C}\left(G_{i,\mathrm{act}} - G_{i,\mathrm{pred}}\right)^2, \tag{4}$$

where C is the number of gas/odor classes, G_{ij} is the number of well-classified samples for $i = j$ and misclassified samples for $i \neq j$. Moreover, $G_{i,\mathrm{act}}$ and $G_{i,\mathrm{pred}}$ are the actual and predicted gas classes.

The use of PC -based padding for efficient classification of gases/odors using a simpler 2D-CNN provides an insight that only the classification task can be achieved with a simpler classifier network and compressed input vectors. With our proposed approach, better classification of gases/odors can be achieved even using zero-padded virtual sensor responses. But the significant enhancement in the performance using PC -based padding is clearly shown in Tab. 4. Moreover, based on the performance enhancement so achieved, other virtual sensor responses can also be used for the generation of the virtual sensor responses by using other normalization and transformation techniques. In this way, with our proposed novel approach we can apply the proposed methods universally.

The insight behind the use of PCA-based non-zero-padding is that it generates all the required virtual sensor responses with inherent ranking carries most of the information in its principal components, which justifies the success of our proposed method. zero-padding, in contrast, is the conventional padding scheme and supplies zero information. On using non-zero-padding (PCs-based padding) the performance enhancement can be seen through each of the used performance assessment metrics. This is further observed that the use of non-zero-padded virtual sensor responses presents more information to the CNN which eventually enhances the classification performance, without actually requiring the need of 16-physical sensor elements. Instead, we have achieved 100 % correct classification results, for both the datasets by using test vectors, which were not used during the training of the CNNs so trained.

5 Conclusion

E-noses, designed using a real-physical multi-element gas sensor array has been an age-old approach in the field of gas/odor classification to achieve high performance. The use of transient and steady responses of the gas sensor array, in conjunction with artificial neural networks and other pattern recognition methods, has also been quite popular. However, with the advent of 6th Generation Internet of Things (6G-IoT) technologies, there is a need to significantly reduce the consumed power in the sensor array while performance is also mandatory. Now with the Intelligence-on-the-edge and computer power on the sensor node, we can also embed CNNs on the sensor node itself. Hence, in our proposed novel approach, we have leveraged the CNNs and by using the upscaled form of sensor responses in the hybrid form, we have been able to achieve very high accuracy in respect of the performance so achieved by the authors who have used the same reference of dataset_1 and dataset_2. Our results surpass the previously published results on the same datasets. We have used the hybrid non-zero virtual sensor response padded approach by using the virtual sensor responses derived from principal component analysis of the curated real-physical responses themselves. It is also evident, that simpler CNNs can perform far better with even much less information, if the same information could be presented with more diversity, such as, in the form of virtual sensor responses, obtained in the form of principal components. Furthermore, our concept of non-zero padding also paves the way to explore other techniques of virtual sensor response generation by using various normalization and transformation techniques. With our proposed novel approach, the high-performance classification of gases/odors has been successfully achieved by using simpler CNNs and by using a much smaller number of real-physical sensors on the sensor nodes. It can also be appreciated that the gas sensor elements contribute to high power requirements on the sensor node and reduction of the number

of real-physical sensor elements significantly reduces the power requirements of the sensor node incurring any loss of performance. To the best of the authors' knowledge, the use of upscaled hybrid sensor responses with principal components as virtual sensor responses for efficient classification of the considered gases/odors has been presented for the first time and the CNN used is also a simpler 2D-CNN.

References

[1] X. Zhai, A. A. S. Ali, A. Amira, and F. Bensaali, "MLP Neural Network Based Gas Classification System on Zynq SoC", *IEEE Access*, vol. 4, pp. 8138–8146, doi: 10.1109/ACCESS.2016.2619181, 2016.

[2] A. Vanarse, A. Osseiran, and A. Rassau, "Real-Time Classification of Multivariate Olfaction Data Using Spiking Neural Networks", *Sensors*, vol. 19, o. 8, pp. 1841, doi: 10.3390/s19081841, 2019.

[3] U. Yaqoob, and M. I. Younis, "Chemical Gas Sensors: Recent Developments, Challenges, and the Potential of Machine Learning: A Review", *Sensors*, vol. 21, no. 8, p. 2877, doi: 10.3390/s21082877, 2021.

[4] W. S. Al-Dayyeni *et al*, "A Review on Electronic Nose: Coherent Taxonomy, Classification, Motivations, Challenges, Recommendations and Datasets", *IEEE Access*, vol. 9, pp. 88535–88551, doi: 10.1109/ACCESS.2021.3090165, 2021.

[5] N. S. Rajput, R. R. Das, V. N. Mishra, K. P. Singh, and R. Dwivedi, "A neural net implementation of SPCA pre-processor for gas/odor classification using the responses of thick film gas sensor array", *Sensors and Actuators B: Chemical*, vol. 148, pp. 550–558, May 2010.

[6] P. Peng, X. Zhao, X. Pan, and W. Ye, "Gas Classification Using Deep Convolutional Neural Networks", *Sensors*, vol. 18, no. 1, p. 157, Jan 2018.

[7] S. Lekha, and M. Sucheta, "Real-Time Non-Invasive Detection and Classification of Diabetes Using Modified Convolution Neural Network", *IEEE Journal of Biomedical and Health Informatics*, vol. 22, no. 5, pp. 1630–1636, doi: 10.1109/JBHI.2017.27575 10, Sep 2018.

[8] S. N. Chaudhri, and N. S. Rajput, "Mirror Mosaicking: A Novel Approach to Achieve High-performance Classification of Gases Leveraging Convolutional Neural Network", *Proceedings of the 10th International Conference on Sensor Networks, SENSORNETS*, vol. 1, pp. 86–91, 2021.

[9] K. A. Ngo, P. Lauque, and K. Aguir, "Identification of Toxic Gases Using Steady-State and Transient Responses of Gas Sensor Array", *Sensors and Materials*, vol. 18, no. 5, pp. 251–260, 2006.

[10] X. Zhao, Z. Wen, X. Pan, W. Ye, and A. Bermak, "Mixture Gases Classification Based on Multi-Label One-Dimensional Deep Convolutional Neural Network", *IEEE Access*, vol. 7, pp. 12630-12637, doi: 10.1109/ACCESS.2019.2892754 2019.

[11] S. I. Choi, T. Eom, and G.-M. Jeong, "Gas classification using combined features based on a discriminant analysis for an electronic nose", *J. Sensors*, Mar 2016.

[12] H. Li, D. Luo, Y. Sun, and H. G. Hosseini, "Classification and Identification of Industrial Gases Based on Electronic Nose Technology", *Sensors*, Basel 19, pp. 5033, 2019.

[13] L. Han, C. Yu, K. Xiao, and X. Zhao, "A new method of mixed gas identification based on a convolutional neural network for time series classification", *Sensors*, vol. 19, no. 9, pp. 1960–1982, 2019.

[14] G. Wei, G. Li, J. Zhao, and A. He, "Development of a LeNet-5 gas identification CNN structure for electronic noses", *Sensors*, vol. 19, no. 1, p. 217, 2019.

[15] Y. Lecun, L. Bottou, Y. Bengio, and P. Haffner, "Gradient-based learning applied to document recognition", *Proceedings of the IEEE*, vol. 86, no. 11, pp. 2278–2324, doi: 10.1109/5.726791, Nov 1998.

[16] A. U. Rehman, S. B. Belhaouari, M. Ijaz, A. Bermak, and M. Hamdi, "Multi-Classifier Tree with Transient Features for Drift Compensation in Electronic Nose", *IEEE Sensors Journal*, vol. 21, no. 5, pp. 6564–6574, doi: 10.1109/JSEN.2020.3041949,.

[17] E. Llobet, J. Brezmes, X. Vilanova, J. E. Sueiras, and X. Correig, "Qualitative and quantitative analysis of volatile organic compounds using transient and steady-state responses of a thick-film tin oxide gas sensor array", *Sens. Actuators B Chem*, vol. 41, no. 1, pp. 13–21, Jun 1997.

[18] S. N. Chaudhri, and N. S. Rajput, "Multidimensional Multiconvolution Based Feature Extraction Approach for Drift Tolerant Robust Classifier for Gases/Odors", *IEEE Sensors Letters*, doi: 10.1109/LSENS.3153832, (Accepted) 2022.

[19] T. Wang, M. Sun, and K. Hu, "Dilated Deep Residual Network for Image Denoising", *IEEE 29th International Conference on Tools with Artificial Intelligence (ICTAI*,), Boston, MA, pp. 1272-1279, doi: 10.1109/ICTAI.2017.00192, 2017.

[20] A. Wu, W. Zheng, H. Yu, S. Gong, and J. Lai, "RGB-Infrared Cross-Modality Person Re-identification", *IEEE International Conference on Computer Vision* (ICCV), Venice, pp. 5390–5399, doi: 10.1109/ICCV.2017.575, 2017.

[21] K. O'Shea, and R. Nash, "An introduction to convolutional neural networks", *CoRR*, abs/1511.08458, 2015.

[22] A. Nguyen, S. Choi, W. Kim, S. Ahn, J. Kim, and S. Lee, "Distribution Padding in Convolutional Neural Networks", *IEEE International Conference on Image Processing* (ICIP), Taipei, Taiwan, pp. 4275–4279, doi: 10.1109/ICIP.2019.8803537, 2019.

[23] A. Mishra, N. S. Rajput, and G. Han, "NDSRT: An Efficient Virtual Multi-Sensor Response Transformation for Classification of Gases/Odors", *IEEE Sensors Journal*, vol. 17, no. 11, pp. 3416-3421, doi: 10.1109/JSEN. 2017.2690536, Jun 2017.

[24] Y. G. Zhang, C. H. Zhang, Y. Zhao, and S. Gao, "Wind speed prediction of RBF neural network based on PCA and ICA", *J. Elect. Eng. Slovak*, vol. 69, no. 2, pp. 148–155, Mar 2018.

[25] S. N. Chaudhri, N. S. Rajput, K. P. Singh, and D. Singh, "Mirror Mosaicking Based Reduced Complexity Approach for the Classification of Hyperspectral Images", *IEEE International Geoscience and Remote Sensing Symposium* (IGARSS), pp. 3657–3660, doi: 10.1109/IGARSS47720.2021.9554276, 2021.

[26] D. Dua, and C. Graff, "UCI Machine Learning Repository", http://archive.ics.uci.edu/ml, *Irvine, CA: University of California, School of Information and Computer Science*, 2019.

[27] J. Fonollosa, L. Fernández, A. Gutiaérrez-Gálvez, R. Huerta, and S. Marco, "Calibration transfer and drift counteraction in chemical sensor arrays using direct standardization", *Sensors Actuators B Chem*, vol. 236, pp. 1044–1053, Nov 2016.

[28] A. Ziyatdinov, J. Fonollosa, L. Fernndez, A. Gutierrez-Glvez, S. Marco, and A. Perera, "Bioinspired early detection through gas flow modulation in chemo-sensory systems", *Sens Actuators B Chem*, vol. 206, pp. 5r38–547, 2015.

Received 1 March 2022